Correlational study between model variables and observable quantities of magnetar-powered H-rich supernovae

N.P. Maffione[1,2], M. Orellana[1,2] & M.C. Bersten[3,4,5]

[1] *Laboratorio de Procesamiento de Señales Aplicado y Computación de Alto Rendimiento, Sede Andina, UNRN, Argentina*
[2] *Consejo Nacional de Investigaciones Científicas y Técnicas, Argentina*
[3] *Instituto de Astrofísica de La Plata, CONICET–UNLP, Argentina*
[4] *Kavli Institute for the Physics and Mathematics of the Universe, The University of Tokyo, Japan*
[5] *Facultad de Ciencias Astronómicas y Geofísicas, UNLP, Argentina*

Contact / npmaffione@unrn.edu.ar

Resumen / Aún no ha sido posible identificar la presencia de un magnetar en una explosión de supernova (SN). Sólo conocemos piezas en un escenario desafiante que nos presenta interrogantes sumamente trascendentes. Si tuviéramos un magnetar con una velocidad de rotación suficientemente alta en una dada SN, este debería contribuir a la misma con una fuente adicional de energía. Esta fuente podría incluso superar la energía liberada por los mecanismos más usuales, dando lugar al nacimiento de una SN superluminosa.
Recientemente se ha construido una grilla de modelos hidrodinámicos (con un tratamiento simple de los procesos radiativos) para un progenitor rico en hidrógeno y masa $M_{ZAMS} = 15\ M_\odot$. Las curvas de luz (LC por sus siglas en inglés) obtenidas muestran evidencia indirecta de las propiedades del magnetar. Por medio de un análisis correlacional sencillo investigamos la existencia de relaciones entre las variables usadas para definir los modelos (energía inicial de rotación y tiempo de frenado) y cantidades observables derivadas de las LCs. Esta clase de estudios podrían ayudar a definir estrategias para la búsqueda de magnetares en SNs con buen seguimiento fotométrico. En este trabajo presentamos algunos resultados preliminares.

Abstract / Up to date, it has not been possible to identify the presence of a magnetar in a supernova (SN) explosion. We know only pieces of a challenging scenario that poses ahead extremely important questions. If a magnetar with a sufficiently high rotation speed is actually present in a given SN, it would contribute as an additional energy source. That power source may overcome the energy released by otherwise usual mechanisms, so a magnetar could give birth to a superluminous SN.
A grid of hydrodynamic models (with a simple treatment for radiative processes) has been recently computed for a hydrogen-rich progenitor of $M_{ZAMS} = 15\ M_\odot$. The corresponding light curves (LCs) show indirect evidence of the properties of the magnetar. By means of a simple correlational analysis, we investigate the existence of a correspondence between the variables used to define the models (initial rotation energy and spin-down timescale) and the observable quantities derived from the LCs. This type of analyisis might help to define search strategies to obtain evidence of the magnetar engine working into SNe, with good photometric data. Herein we present some preliminary results.

Keywords / supernovae : general — stars : magnetars — methods : statistical

1. Introduction

It has been suggested that some supernovae (SNe) may be powered by a magnetar formed at the moment of the explosion. The additional energy provided by the magnetar may result in an extra bright light curve (LC). In the context of hydrogen-rich (H-rich) progenitors, magnetar powered LCs have not been deeply studied in the literature (Bersten & Benvenuto, 2016; Orellana et al., 2018, and references therein). We investigate here the correlation matrices between intrinsic properties (parameterized with model variables) of an hypothetical magnetar and plausible observable quantities from the LC. Our goal is to test the connection between these two types of data.

2. Numerical model and model variables

A grid of hydrodynamic models (with a simple treatment for radiative processes) has been computed for an H-rich progenitor, with the following characteristics: (a) main sequence mass of 15 $M_\odot$ consistently evolved until core collapse by Nomoto & Hashimoto (1988), (b) the pre-SNe model shows a transition between H-rich to He-rich at a layer of $\simeq 3.2\ M_\odot$, (c) the pre-explosion radius is 500 $R_\odot$ and (d) the surface metallicity is $Z \sim 0.02$. To parameterize the magnetar source, Orellana et al. (2018) used the spin-down timescale (t_p) and the initial rotation energy (E_{rot}) as the model free parameters (hereinafter MFPs). In Fig. 1 we present the corresponding bolometric LCs. In the presence of a magnetar, an early short phase of increasing luminosity precedes the maximum (in some cases, the maximum is a plateau). Ac-

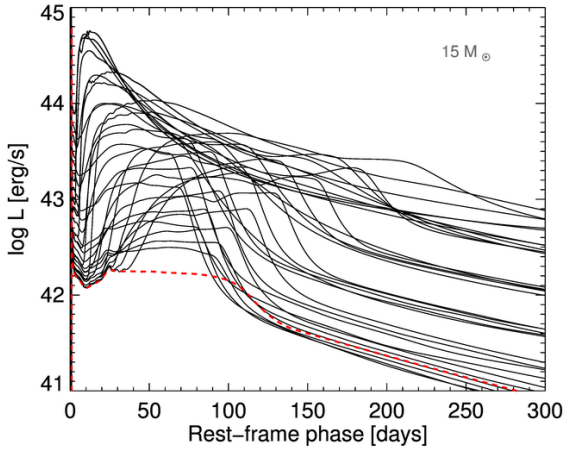

Figure 1: Bolometric LCs for the grid of hydrodynamic models. For comparison, we show the same SN model without a magnetar in red dashed line.

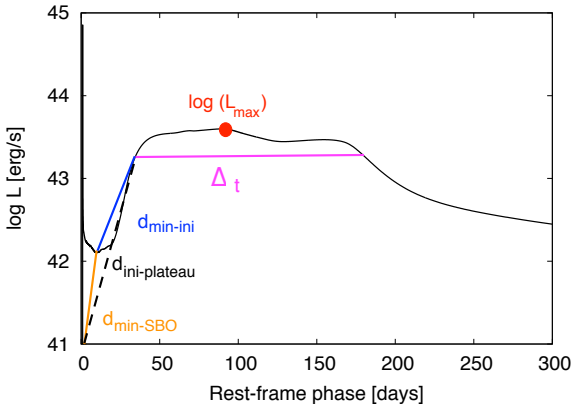

Figure 2: Definition of plausible observables. (a) In red, $\log(L_{max})$: the mean value of the local maxima produced after the shock peak and (b) in purple, Δ_t: which characterizes its duration. Also, the newly defined (i) in orange, $d_{min-SBO}$: the normalized distance of the minimum point after the shock break-out; (ii) in black dashed line, $d_{ini-plateau}$: the normalized distance of the initial point of the plateau phase (defined by the intersection of Δ_t with the light curve) and (iii) in blue, $d_{min-ini}$: the normalized distance between the minimum point after the shock break-out and the initial point of the plateau phase.

cording to these results, the LC is much steeper during this rise than in the case without the magnetar, producing a larger luminosity variation. This seems to be a unique characteristic of the magnetar models that can help us to identify such power source.

3. Definition of observable quantities

For a quantitative study of the LCs we follow Orellana et al. (2018) and use a set of own-defined quantities obtained from the bolometric LCs (see an example in Fig. 2). This set is composed of two quantities introduced in that paper, namely (a) $\log(L_{max})$: the mean value of the local maxima produced after the shock peak and (b) Δ_t: the time interval over which $\log(L) > \log(L_{max}) - 0.2$ dex (or the plateau duration). We introduce three new quantities, measured in the same plane: (i) $d_{min-SBO}$: the normalized distance of the minimum point after the shock break-out (where the normalization is with respect to the scale of the plot and the origin in time is associated with the energy injection that produce the SN), (ii) $d_{ini-plateau}$: the normalized distance of the initial point of Δ_t and (iii) $d_{min-ini}$: the normalized distance between the minimum point after the shock break-out and the initial point of the plateau phase. Whether these are plausible observables depends strongly on the photometric follow up of the SN.

Now we are in position to study the existence of connections among the MFPs and our plausible observables (POs). In next section we compute the corresponding Spearman and Pearson correlation matrices.

4. Correlation matrices

The Spearman correlation matrix (indicative of a monotonic relationship) among the MFPs: t_p and E_{rot} and the set of POs presents the largest values for the following subset of parameter-observable (MFP-PO) pairs: t_p with $d_{min-ini}$ (0.92) and E_{rot} with Δ_t (-0.85) and $\log(L_{max})$ (0.88) and $d_{min-SBO}$ (0.89) and $d_{ini-plateau}$ (0.84). Notice that a negative Spearman coefficient means a monotonic function that reverse order, while a positive coefficient preserves order. All Spearman coefficients are rather large which means strong evidence of a monotonic function behind the MFP-PO pairs from the subset.

In Fig. 3 we present the Pearson correlation matrix (indicative of a linear relationship) for the complete set of parameters and observables, to visualize if there is further indication of a stronger dependence (i.e. not only monotonic but linear) among such quantities. Blue and red pies (below the main diagonal) correspond to a positive and negative slope, respectively. Scatter plots (above the main diagonal) are also included in order to visualize the actual distribution of the data. The aforementioned subset of MFP-PO pairs (i.e. those with the largest values of the Spearman coefficient) are framed in the figure, with their Pearson coefficient also included. Rather large (absolute) values of the Pearson coefficient are observed for almost every pair from the selected subset.

Notice the strong linear dependence (according to their Pearson coefficient, ~ 1) between two of the POs: $\log(L_{max})$ and $d_{ini-plateau}$ which means that they can be used interchangeably.

4.1. Connecting the model variables with the observable quantities

From the subset of MFP-PO pairs, we kept those with the largest Spearman and/or Pearson coefficients. For instance, the pair (t_p, $d_{min-ini}$) has the largest Spearman coefficient (0.92) and the only one from the sample that includes the MFP t_p and has an (absolute)

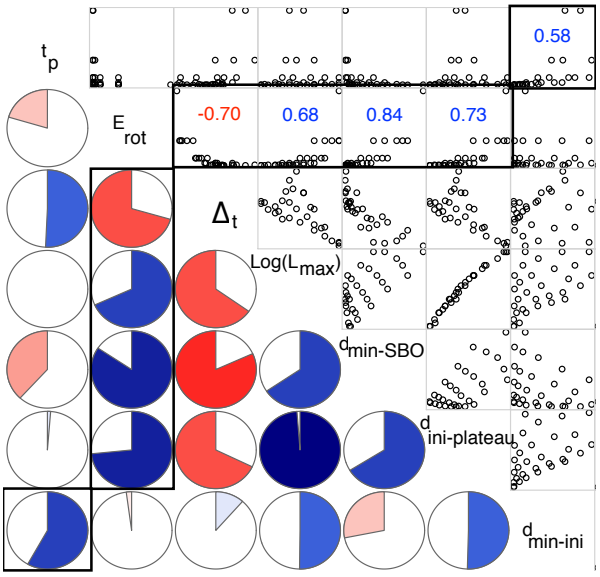

Figure 3: Pearson correlation matrix (indicative of a linear relationship) for the complete set of parameters and observables under study. The subset of parameter-observable pairs with the largest values of the Spearman coefficient is framed and the value of their Pearson coefficient is also included.

value of the Spearman coefficient larger than 0.7. On the other hand, the MFP E_{rot} has large values of the Spearman coefficient for many of the selected POs, being the largest (0.89), the one associated with the pair (E_{rot}, $d_{min-SBO}$). Their Pearson coefficient is also large ($\sim$ 0.84, see Fig. 3). However, there is some level of unwanted degeneracy in their relationship as it can be seen from the middle panel of Fig. 4, where we present two candidates for suitable MFP-PO pairs to re-parameterize the grid of hydrodynamic models (Section 2.). The second largest Spearman coefficient (0.88) is for (E_{rot}, $\log(L_{max})$). The latter also presents a rather large Pearson coefficient, $\sim$ 0.68. The bottom panel of Fig. 4 shows the behavior of such election in re-parameterizing the grid. There is no sign of degeneracy, thus probing to be the most suitable MFP-PO pair.

5. Conclusions and forthcoming research

By means of a correlational analysis we found the existence of a possible one-to-one correspondence (with rather large Spearman and Pearson coefficients) between the free parameters used to define the models (spin-down timescale and initial rotation energy of the magnetar) and a couple of own-defined (and plausible observable) quantities. Such pair of observable counterparts extracted from the synthetic light curves is given by $d_{min-ini}$ and $\log(L_{max})$. The former component can be difficult to observe, though. Then, we are evaluating the possibility to replace that observable with another one easier to detect.

Acknowledgements: This research was partially supported by PI2017-40B531 of Universidad Nacional de Río Negro.

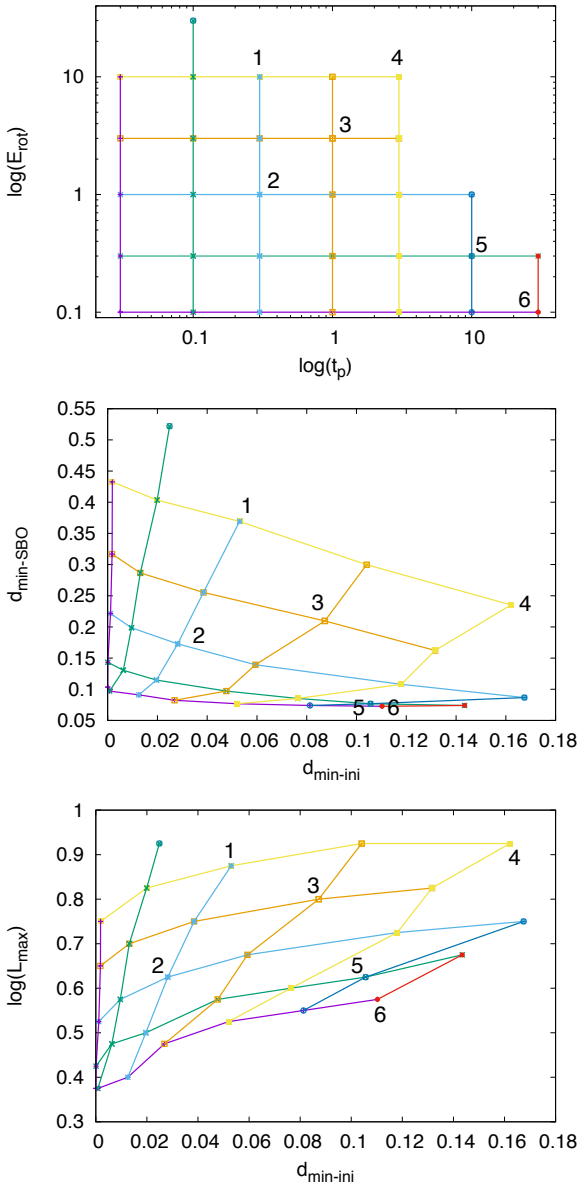

Figure 4: Examples of parameter-observable pairs. Top panel: grid of hydrodynamic models parameterized by model free parameters: spin-down timescale (t_p) and the initial rotation energy (E_{rot}) of the magnetar (in log scale). Middle panel: re-parameterization of the grid by two of our own-defined observables: $d_{min-ini}$ and $d_{min-SBO}$. Bottom panel: idem middle panel but using the following observables: $d_{min-ini}$ and $\log(L_{max})$. The bottom panel shows a parameter-observable pair satisfying a one-to-one relation: there is no sign of degeneracy in the transformation (see the correspondence of the colours in the electronic version, or the numbered points in the B&W printed version of the paper).

References

Bersten M.C., Benvenuto O.G., 2016, BAAA, 58, 246
Nomoto K., Hashimoto M., 1988, PhR, 163, 13
Orellana M., Bersten M.C., Moriya T.J., 2018, A&A, 619, A145